

Predictive Feedback Control Method for Stabilization of Continuous Time Systems

Lina A. Shalby^{1,2}

¹*Moscow Institute of Physics and Technology, Dolgoprudny, Moscow Region, Russia*

²*Faculty of Women, Ain Shams University, Cairo, Egypt*

Abstract: Recent researchers have studied the chaotic phenomenon and introduced methods to control chaos. One of these methods is the Predictive Feedback Control (PFC). PFC method has been used to stabilize only the discrete chaotic maps. In this paper, we generalize the PFC method by extending it to stabilize continuous time systems. The numerical simulations are carried out to solve the system using Euler method for its simplicity, and then the PFC method is applied to the discretized system. The controlled trajectory converges to an unstable equilibrium point via small control action. The stability analysis is shown compared to that of the continuous system in details. Also the choice of the controlling input of the PFC method and its properties are discussed. Lorenz system and Rössler system are the well known chosen chaotic examples. The PFC method is applied to each of them, showing stability at each of their equilibrium point. With a very small control, the behaviour of the system is completely changed from chaos to stable.

Keywords: Continuous time systems, chaos control, Euler method, Predictive feedback control, Unstable equilibrium point

1. INTRODUCTION

Chaos theory is one of the recent fields of study that attracts the interest of scientists. Two most important properties of chaos are the high sensitivity of trajectories to initial conditions and to parameter values. In the last decades, many researchers concerned with how to control chaotic phenomena depending on these two properties. They aimed to bring a trajectory to a small neighborhood of a desired location in the chaotic attractor, using a small perturbation. Pioneering work Ott-Grebogi-Yorke [12] proposed OGY method for stabilizing chaos. It could only be applied to discrete data, so continuous time systems should first be made discrete time by using the Poincare map. Then it was followed by many other publications adjusting and extending the OGY method as in [6] and [7], see also survey [1]. Pyragas [14, 15] proposed the delayed feedback control (DFC) to stabilize the unstable periodic orbits (UPO). The control input was given as the multiplication of a gain with the difference between current system state and a state with the time delay as it is discussed in [4]. DFC method is firstly constructed for continuous time systems and extended to the discrete-time case in [18]. Many applications, such as in [3, 10], were controlled by using DFC method. Also, many developments for DFC method were performed, see [8, 11]. One of the recent surveys on DFC is presented in [16].

Ushio [19] introduced the idea of predicting control in his paper and it was extended in [2] to stabilize continuous time systems using predictive-based control method. Predictive

*Corresponding author: lina.khamis@gmail.com, Lina.Khamis@women.asu.edu.eg

Feedback Control (PFC) [13] is an easily implemented method to stabilize unknown UPOs in discrete time dynamical systems. In PFC, the control input was given as the multiplication of a gain with the difference between two predicted future system states. PFC depends on applying small controls that completely change the nature of system's behavior and devotes its attention to the most important problem of stabilizing or controlling chaos. Detailed survey on existing approaches and methods for chaos control can be found in the Handbook of Chaos Control [17].

In the next section of the paper, we extend PFC to stabilize chaotic continuous time dynamical systems solved numerically by Euler method and the PFC method is analyzed. In section 3, the numerical simulations results are given for the most popular examples of chaos: Lorenz system and Rössler system.

2. PREDICTIVE FEEDBACK CONTROL METHOD

We start with introducing the PFC method [13] for discrete-time system which depends on the system state and a control action $u(x)$ as follows

$$x_{n+1} = F(x_n) - u(x_n), \quad (2.1)$$

where $F, u : \mathbb{R}^N \rightarrow \mathbb{R}^N$ and $u(x) = E(F^{p+2}(x) - F^{p+1}(x))$, for a chosen control gain matrix E and any arbitrary forward predicted state p ($p > 0$), by denoting $F^{p+1}(x) = F(F^p(x))$, $F^1(x) = F(x)$ — prediction of the map F for $p + 1$ iterations forward. The idea is to choose E to stabilize unstable orbits or unstable equilibria points via small control action $u(x)$. Indeed state x and control u are of the same dimension N , and this strongly limits the application of the proposed technique to real-life problems. However there are various situations where such controls are applicable. For instance if one deals with classical analytical examples (e.g. Rössler and Lorenz systems) it is of interest to deal with their fixed points and orbits which are unstable. Then PFC allows to stabilize such points and orbits. And the main peculiarity of the approach is the arbitrary small control action required. Suppose $N = 1$, x^* is an unstable equilibria point point of $F(x)$, that is $x^* = F(x^*)$, $\mu = |F'(x^*)| > 1$. Then for $E = \frac{1}{\mu^{p+1}(\mu-1)}$, iterations of (1) converge to x^* . The most important fact is obtaining control $u(x)$ small enough. Indeed, if we deal with chaos control, iterations $F^p(x)$ remain bounded, while E is small for p large, because $\mu > 1$. It is effective to choose p large enough (because larger is p , smaller is the control action). However, large predictive horizons imply computational error. Thus the choice of p is some trade-of. In [13] the result is extended for $N > 1$ and for unstable orbits (i.e. for x^* such that $x^* = F^k(x^*)$ with $k > 1$). Similar results are available for μ known approximately.

The goal of the present paper is the application of the above results for continuous-time systems. Let us consider a system of nonlinear autonomous differential equations

$$\dot{x} = f(x), \quad (2.2)$$

where $x \in \mathbb{R}^N$, and f is assumed to be differentiable. An equilibrium point x^* necessarily satisfies $f(x^*) = 0$. The following result on asymptotic stability is standard (see e.g. [5]). The equilibrium point $x = x^*$ of $\dot{x} = f(x)$ is asymptotically stable if all eigenvalues of the Jacobian matrix $A = f'(x^*)$ satisfy $Re(\lambda_i) < 0$.

From now on, we reduce a continuous time system to a discrete time map. This map is created from sampling the flow at discrete times $t_n = t_0 + nh$, $n = 0, 1, 2, \dots$, where the sampling interval h can be chosen on the basis of convenience. Thus, a continuous time trajectory $x(t)$ yields a discrete time trajectory $x_n = x(t_n)$. By using Euler method, the simplest numerical method to solve a differential equation, the system will be discretized easily to take the form

$$x_{n+1} = x_n + hf(x_n) = F(x_n), \quad (2.3)$$

where $F(x) = x + hf(x)$. Equation (2.3) is the simplest discrete form corresponding to the continuous time system. Lemma 2.1 highlights the relation between the discretized function F and the continuous system function f . Let μ_i denote the eigenvalues of the Jacobian matrix $M = F'(x^*) = I + hf'(x^*)$, $f(x^*) = 0$, while λ_i are eigenvalues of $A = f'(x^*)$.

Lemma 2.1:

$F(x)$ satisfies the following:

(i) $F(0) = 0$, and $F(x^*) = x^* + hf(x^*) = x^*$.

(ii) Let $Re(\lambda_i) = u_i$ and $Im(\lambda_i) = \nu_i$, if $u_i < 0$ and $0 < h < \frac{2|u_i|}{u_i^2 + \nu_i^2}$, then $|\mu_i| = |1 + hu_i| < 1$, and if $u_i \geq 0$, then $|\mu_i| \geq 1$.

Lemma 2.1 shows that the discrete form for the continuous system has the same equilibrium point, and unstable equilibrium points of the continuous system imply instability of the discrete system. Thus for the discretized system, the predictive feedback control method in [13] can be used to stabilize the system as illustrated for the vector case. Thus we arrive to the following stabilization scheme for continuous system (2), where the matrix E could be considered to be the diagonal with entries ϵ_i . The choice of ϵ_i depends on the value of the eigenvalues μ_i of the Jacobian matrix M , which could be real or complex. Firstly, for $|\mu_i| < 1$, we take $\epsilon_i = 0$. Secondly, if $|\mu_i| \geq 1$ and $\mu_i \in \mathbb{R}$, then $\epsilon_i = \frac{1}{\mu_i^{p+1}(\mu_i-1)}$. Thirdly, if $|\mu_i| \geq 1$ and $\mu_i \in \mathbb{C}$, such that $\mu_i = a_i + b_i j$, $j = \sqrt{-1}$, then the control input ϵ_i will be a 2×2 matrix: $\epsilon_i = D^{-p-1}(D - I_2)^{-1}$, where $D = \begin{bmatrix} a_i & b_i \\ -b_i & a_i \end{bmatrix}$. We restrict our analysis with fixed points, because orbits are fixed points of the iterated maps. The next theorem and its proof illustrate local stability of the system for these choice of the control gain.

Theorem 2.1:

Let $f \in C^1$, $x \in \mathbb{R}^N$ and assume x^* is an unstable equilibrium point of continuous system (2.2) and its Jacobian matrix M is not Hurwitz. Then x^* is stable fixed point of the predictive feedback control equation (2.1) after discretizing system (2.2) numerically by using Euler method (2.3) provided h is small enough.

Proof

At $x = x^*$, matrix A has eigenvalues λ_i , with $u_i = Re(\lambda_i) > 0$ for some i . Suppose that $F(x)$ is h -step sized Euler approximation of Equation (2.2), given by Equation (2.3), then the Jacobian matrix M has the eigenvalues $\mu_i = 1 + h\lambda_i$. By the chain rule, the Jacobian matrix of $F^p(x)$ is associated with the eigenvalues μ_i^p . Let J is the Jacobian matrix of the right hand side in Equation (2.1) at $x = x^*$, which will have the form, $J = M - E \{M^{p+2} - M^{p+1}\} = M - EM^{p+1} \{M - I\}$,

and J has eigenvalues η_i , $i = 1, \dots, N$. Then $|\eta_i| = |\mu_i - \delta \{\mu_i - 1\}| < 1 \forall i$, for the following cases of μ_i :

For all $|\mu_i| < 1$, $\epsilon_i = 0$ and $\eta_i = \mu_i$.

If $|\mu_i| \geq 1$ and $\mu_i \in \mathbb{R}$, for $\epsilon_i = \frac{\delta h |\lambda_i|}{\mu_i^{p+1}(\mu_i-1)} = \frac{\delta}{\mu_i^{p+1}}$, $1 < \delta < \frac{1}{h|\lambda_i|}$, then $|\eta_i| = |\mu_i - \delta(\mu_i - 1)| = |1 + h\lambda_i - \delta h \lambda_i| = |1 - (\delta - 1)h\lambda_i| < 1$.

While if $|\mu_i| \geq 1$ and $\mu_i \in \mathbb{C}$, for $\epsilon_i = \delta h |\lambda_i| (D^{-p-1}(D - I_2)^{-1})$, $1 < \delta < \frac{1}{h|\lambda_i|}$ where

$D = \begin{bmatrix} a_i & b_i \\ -b_i & a_i \end{bmatrix}$ has the same eigenvalues μ_i and D^p has the eigenvalues μ_i^p . Then $|\eta_i| =$

$|\mu_i - \frac{\delta h |\lambda_i|}{\mu_i^{p+1}(\mu_i-1)} \mu_i^{p+1}(\mu_i - 1)| = |1 + h\lambda_i - \delta h |\lambda_i|| < 1$.

Hence the system is stable since the eigenvalues of J are less than unity. □

The next section illustrates the examples of chaotic systems and their stabilization achievement after adding the control term. The examples are clearly showing easy implementation and the efficiency of the PFC method.

3. EXAMPLES

In this section, we provide two examples of the PFC method applied to classical chaotic system. Lorenz model is 3D system example, and Rössler system is 4D example.

3.1. Lorenz Model

Lorenz [9] was the first who introduced the strange attractor notion and coined the term “butterfly effect”. Lorenz system is described by differential equations

$$\begin{aligned}\dot{x} &= -\sigma(x - y) \\ \dot{y} &= -xz + rx - y \\ \dot{z} &= xy - kz\end{aligned}\quad (3.4)$$

Equation (3.4) has two nonlinear terms, and exhibits both periodic and chaotic motion depending upon the values of the control parameters σ , r and k . By using Euler method the system will be discretized to the form

$$\begin{aligned}x_{n+1} &= x_n - h\sigma(x_n - y_n) \\ y_{n+1} &= y_n + h(-x_n z_n + r x_n - y_n) \\ z_{n+1} &= z_n + h(x_n y_n - k z_n)\end{aligned}\quad (3.5)$$

where h is the step size for discretization of time t . The stability analysis of Equation (2.1) can be performed by studying the discrete 3D function corresponding to it,

$$F(x, y, z) = \begin{cases} x - h\sigma(x - y) \\ y + h(-xz + rx - y) \\ z + h(xy - kz). \end{cases}\quad (3.6)$$

The system (3.4) has three fixed points $s_1 = (-b\sqrt{r-1}, -b\sqrt{r-1}, r-1)$, $s_2 = (0, 0, 0)$ and $s_3 = (b\sqrt{r-1}, b\sqrt{r-1}, r-1)$, which are the same as the equilibrium points of the continuous system (we denote 3D vector (x, y, z) as s). Set $\sigma = 10$ and $k = 2.67$, and make r the adjustable control parameter. Varying the values of r reveals a critical value at $r_c = 24.74$. Below r_c the system decays to steady, non-oscillating, state. Once r increases beyond r_c , the continuous oscillatory behavior occurs and the system shows aperiodic behavior which Lorenz called deterministic non-periodic flow which refer to chaos. For $r = 28$, the chaotic case, the equilibrium points are $s_1 = (-8.4906, -8.4906, 27)$, $s_2 = (0, 0, 0)$ and $s_3 = (8.4906, 8.4906, 27)$ and the eigenvalues corresponding to them are $\lambda_{s_1} = \lambda_{s_3} = \{-13.8569, 0.0934 \pm 10.2001j\}$ and $\lambda_{s_2} = \{-22.8277, 11.8277, -2.67\}$. Let us use the step size h to be a small value equal to 0.001 which satisfies the condition due to the complex value of λ_{s_1} (i.e $h < \frac{2 \times 0.0934}{(0.0934)^2 + (10.2001)^2} = 0.00179$), and then the solution of the system is chaotic as shown in Fig. 3.1.

For the discrete form, the eigenvalues are $\mu_{s_1} = \mu_{s_3} = \{0.9861, 1.00009 \pm 0.0102j\}$ and $\mu_{s_2} = \{0.99733, 1.0118, 0.9771\}$. The complex eigenvalues have the absolute value 1.00014. Let us choose $p = 5$, the initial condition to be $(5, 5, 5)$, and step size $h = 0.001$. Starting with stabilizing the system at the origin, at which $\epsilon_1 = \epsilon_1 = 0$ for $|\mu_{s_2}^{(1,3)}| < 1$, and otherwise we

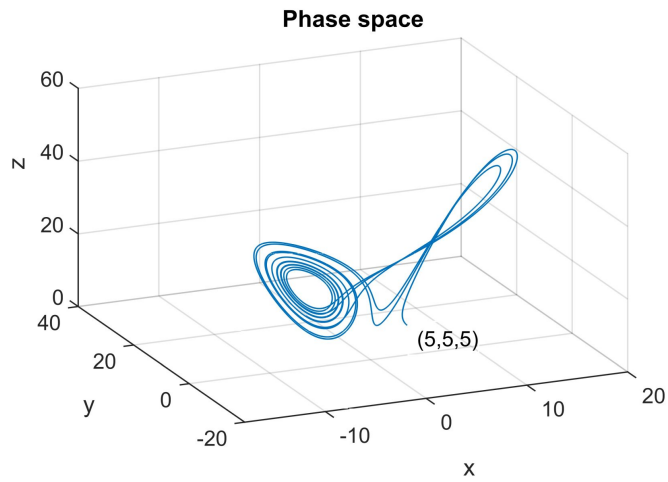


Fig. 3.1. Phase space plot for Lorenz system.

choose $\delta = 2$, $\epsilon_2 = \frac{2}{(\mu_{s_2}^{(2)})^{p+1}}$. The matrix E is taken to be in the form $E = \begin{bmatrix} 0 & 0 & 0 \\ 0 & 1.8638 & 0 \\ 0 & 0 & 0 \end{bmatrix}$ and the first iterate of the decaying additive control term is -0.2040 .

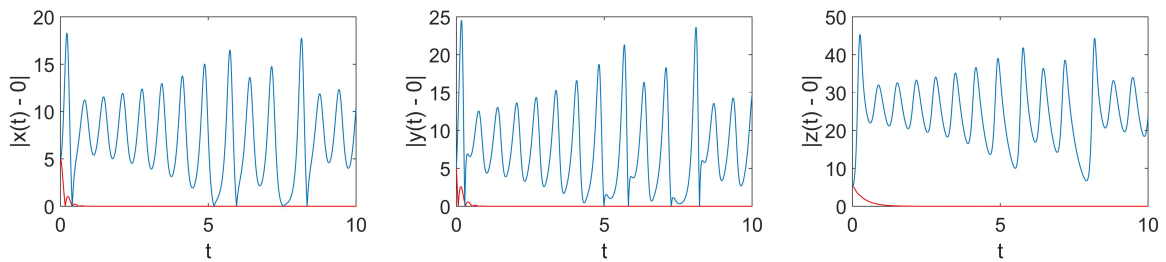


Fig. 3.2. The distance between s and 0 before and after stabilization.

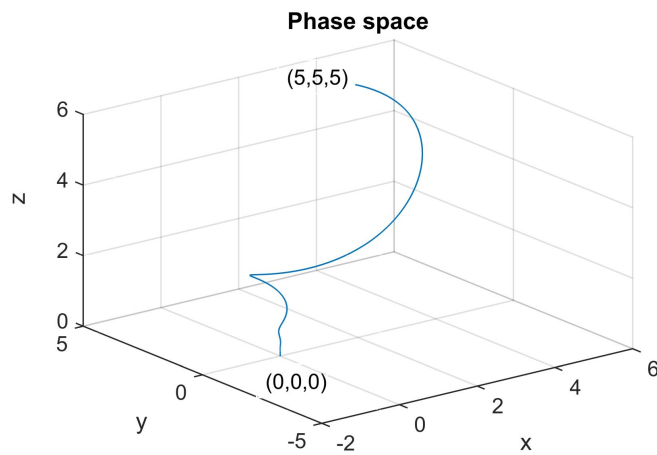


Fig. 3.3. Phase space plot of the controlled trajectory.

Fig. 3.2 illustrates the difference between the equilibrium $(0, 0, 0)$ and the values of x -trajectory, y -trajectory and z -trajectory respectively, before stabilizing the system in blue color compared to those after applying the controlling term to the system that is coloured by red. Fig. 3.3 is the phase space plot of the stabilized system. Both figures show that the system is stable and all variables time series are converging to the origin starting from initial point $(5, 5, 5)$.

In case of the complex eigenvalues, $\mu_{s1}^{(1)} = \mu_{s2}^{(1)} = 0.9861$ and $\mu_{s1}^{(2)} = 1.00009 \pm 0.0102j$, $\epsilon_1 = 0$, and $D = \begin{bmatrix} 1.00009 & 0.01020 \\ -0.01020 & 1.00009 \end{bmatrix}$, $\epsilon_{2,3} = \delta h \mid \lambda_{2,3} \mid D^{-p-1}(D - I_2)^{-1} = \begin{bmatrix} 0.01030 & -0.1978 \\ 0.1978 & 0.01030 \end{bmatrix}$, and $E = \begin{bmatrix} 0 & 0 & 0 \\ 0 & 0.0103 & -0.1978 \\ 0 & 0.1978 & 0.0103 \end{bmatrix}$.

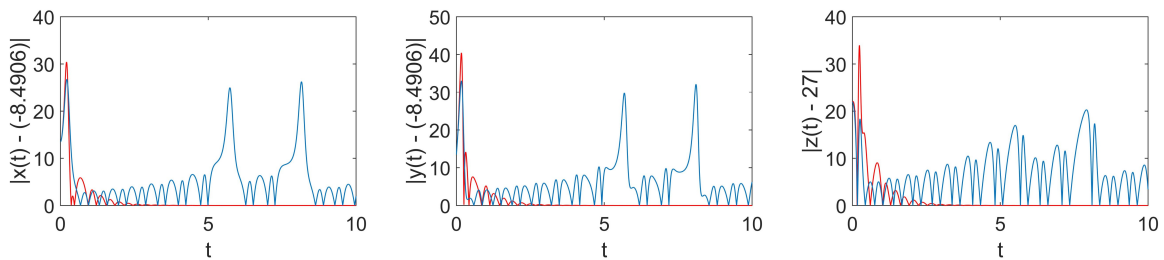


Fig. 3.4. Comparison between the controlled and chaotic trajectories for the equilibrium point $(-8.4906, -8.4906, 27)$.

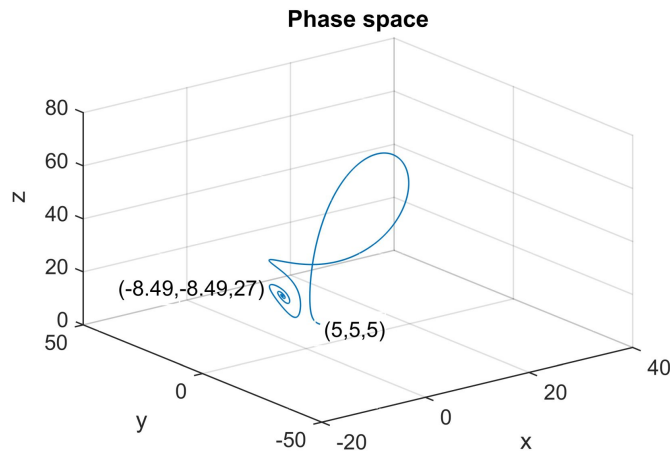


Fig. 3.5. Phase space plot for the controlled trajectory for the equilibrium point $(-8.4906, -8.4906, 27)$.

In Fig. 3.4 and Fig. 3.5, the equilibrium point $(-8.4906, -8.4906, 27)$ is stable. To stabilize the system at $(8.4906, 8.4906, 27)$, the negative sign of the imaginary part of the complex eigenvalue is reversed, so that the matrix D will be $\begin{bmatrix} 1.00009 & -0.01020 \\ 0.01020 & 1.00009 \end{bmatrix}$.

Both Fig. 3.6 and Fig. 3.7 show the slow convergence of the trajectory after stabilization due to the point $(8.4906, 8.4906, 27)$. It is important and interesting to test the effect of different initial conditions. For 50 random initial conditions, the convergence has been tested. At $t = 10$, the trajectories succeeded to reach the fixed points $(0, 0, 0)$ (see Fig. 3.8)

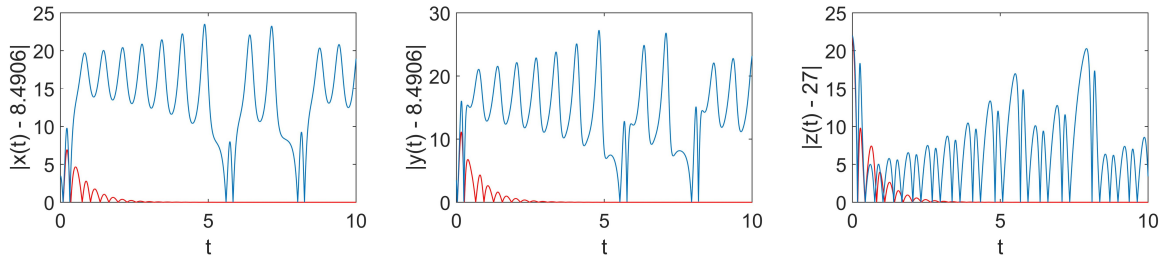


Fig. 3.6. Comparison between the controlled and chaotic trajectories with respect to each dimension with the equilibrium point (8.4906, 8.4906, 27).

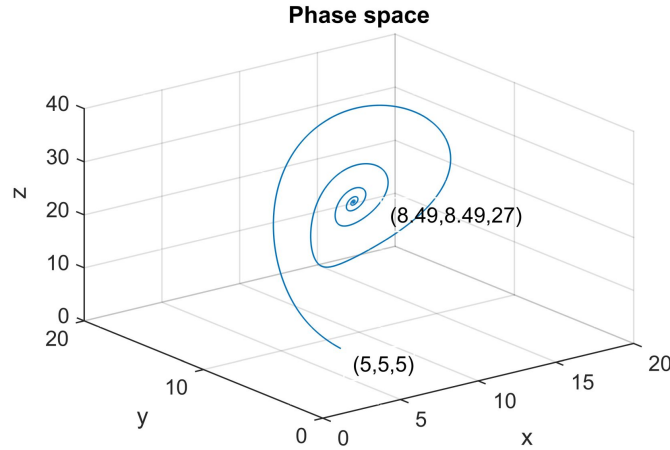


Fig. 3.7. Phase space plot for the controlled trajectory due to the equilibrium point (8.4906, 8.4906, 27).

and (8.4906, 8.4906, 27) (as shown in Fig. 3.9) for all initial points $x_0, y_0 \in [-10, 10]$ and $z_0 \in [0, 30]$.

All the statements rely on local analysis. But in some cases, there was an effect similar to global stabilization, as it is seen in Fig. 3.8 and Fig. 3.9. This fact is a motivation for research of global behavior in future works.

3.2. Rössler Model

Rössler model of 4D phase space is one of the most famous hyperchaos models. For $x \in \mathbb{R}^4$, its defining equations are

$$\begin{aligned}
 \dot{x} &= -y - z \\
 \dot{y} &= x + \alpha y + w \\
 \dot{z} &= \beta + xz \\
 \dot{w} &= -\gamma z + \tau w
 \end{aligned}
 \tag{3.7}$$

The chaotic behavior of the system (3.7) is observed for the parameter values $\alpha = 0.25, \beta = 3, \gamma = 0.5$ and $\tau = 0.05$. In this case, the equilibrium points are $eq1 = (5.40833, 0.55470, -0.55470, -5.54700)$ and $eq2 = (-5.40833, -0.55470, 0.55470, 5.54700)$, which are associated with the eigenvalues $\lambda_{eq1} = \{5.504039, 0.103929, 0.0501791 \pm 0.971052j\}$ (the step size h must be less than 0.1061) and $\lambda_{eq2} = \{0.101890, 0.0493731 \pm 0.9986873j, -5.308963\}$ (the step size h must be less than 0.0987) respectively. By solving the system with Euler method,

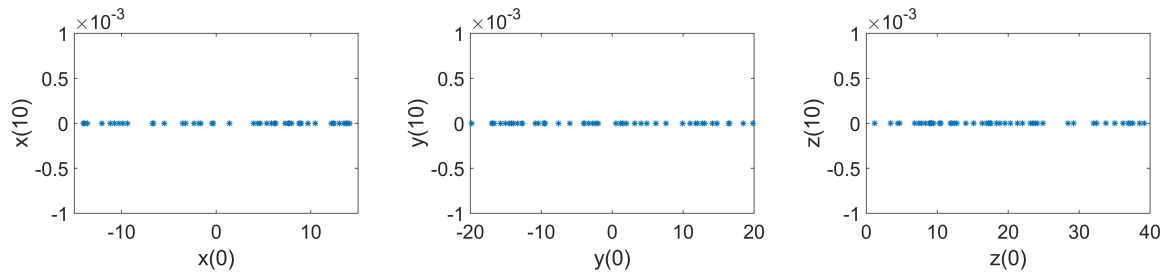


Fig. 3.8. The stability is reachable at $(x(10), y(10), z(10)) = (0, 0, 0)$ for 50 random initial conditions.

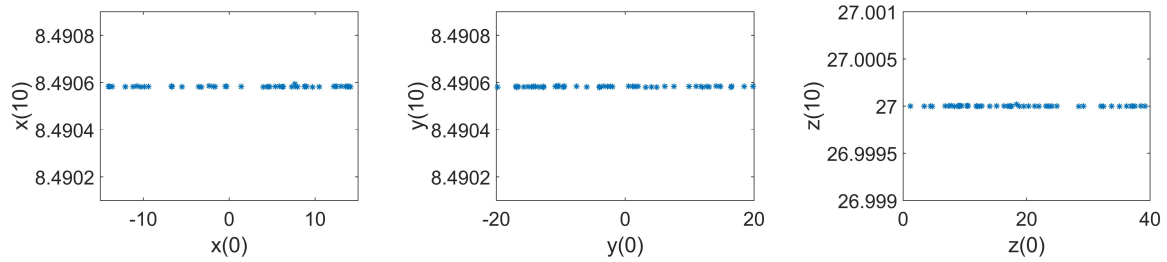


Fig. 3.9. The stability is reachable at $(x(10), y(10), z(10)) = (8.4906, 8.4906, 27)$ for 50 random initial conditions.

adjusting the step size $h = 0.001$ (suitable for stability conditions stated in Lemma 2.1), the continuous system translated to the discrete form with eigenvalues $\mu_{eq1} = \{1.005504, 1.000103929, 1.00005017 \pm 0.00097105j\}$ and $\mu_{eq2} = \{1.000101890, 1.000493731 \pm 0.0009986873j, 0.9946910\}$. Let us use the initial condition $(-10, -6, 0, 10)$, then the system (3.7) is hyperchaos as shown in Fig. 3.10 and Fig. 3.11 for the phase space xyw and $x - y$ plot, respectively.

By setting $p = 3$, $\delta_{1,2} = 1.5$ and $\delta_{3,4} = 5$ for $\epsilon_1 = \frac{\delta_1}{(\mu_{eq1}^{(1)})^4} = 1.46743$, $\epsilon_2 = \frac{\delta_2}{(\mu_{eq2}^{(2)})^4} = 1.49937$, and $\epsilon_{3,4} = \delta_{3,4} \times h \times |\lambda_{eq1}^{(3)}| \times D^{-4} (D - I_2)^{-1} = \begin{bmatrix} 0.01243 & 0.26011 \\ -0.26011 & 0.01243 \end{bmatrix}$, then

$$E_{eq1} = \begin{bmatrix} 0.01243 & 0.26011 & 0 & 0 \\ -0.26011 & 0.01243 & 0 & 0 \\ 0 & 0 & 1.46743 & 0 \\ 0 & 0 & 0 & 1.49937 \end{bmatrix}. \text{ While } \delta_1 = 1.5 \text{ and } \delta_{2,3} = 40 \text{ for}$$

$$\epsilon_1 = \frac{\delta_1}{(\mu_{eq1}^{(1)})^4} = 1.49939, \quad \epsilon_{2,3} = \delta_{2,3} \times h \times |\lambda_{eq2}^{(2)}| \times D^{-4} (D - I_2)^{-1} = \begin{bmatrix} 0.09053 & 1.99260 \\ -1.99260 & 0.09053 \end{bmatrix},$$

$$\text{then } E_{eq2} = \begin{bmatrix} 0.09053 & 1.99260 & 0 & 0 \\ -1.99260 & 0.09053 & 0 & 0 \\ 0 & 0 & 0 & 0 \\ 0 & 0 & 0 & 1.49939 \end{bmatrix}.$$

The first iterate of the control term values are $-0.00031, -0.00158, 0.00419$, and 0.00074 to stabilize the system at eq1. And its first iterate values to stabilize the system at eq2 are $-0.00237, -0.01207, 0$, and 0.00074 . The control term values are small negligible in the real life applications but they are enough to change the behavior of the system from ergodicity to be stable. Fig. 3.12 and Fig. 3.13 are showing the controlled phase space xyw due to eq1 and eq2, respectively. And Fig. 3.14-3.17 are the trajectories convergence of x, y, z and w to the equilibrium points compared to the uncontrolled trajectories, respectively.

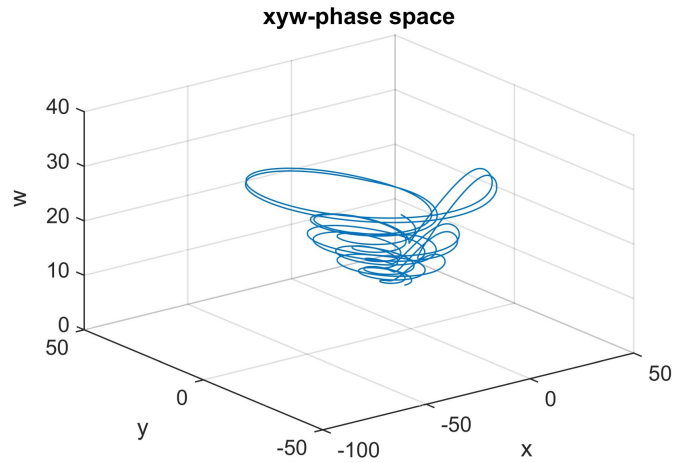


Fig. 3.10. The strange attractors of Rössler hyperchaos system - xyw phase space plot.

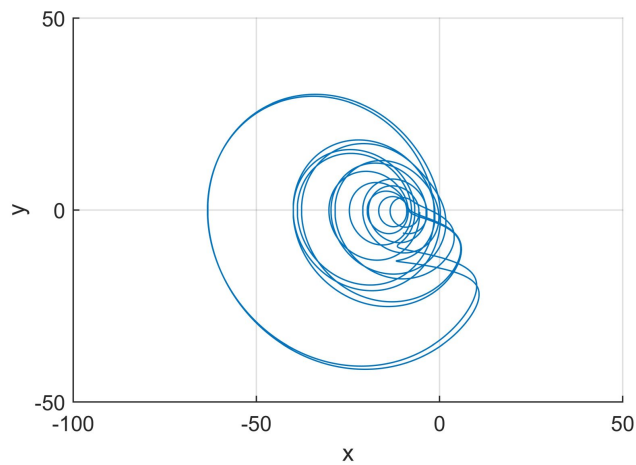


Fig. 3.11. $x - y$ plot for Rössler hyperchaos system.

For each example, the PFC method is successfully stabilized all the equilibrium points. It is also important to discuss the relation between the continuous system and its discretized form numerically, as they are difficult to be solved analytically. At this point, a question may arise. What is the continuous system that has stable attractor while its numerical solution is chaotic?

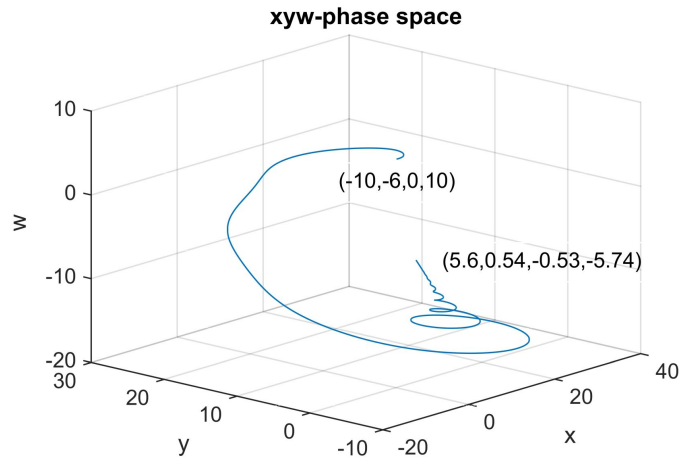


Fig. 3.12. The xyw phase space after control at $eq1$.

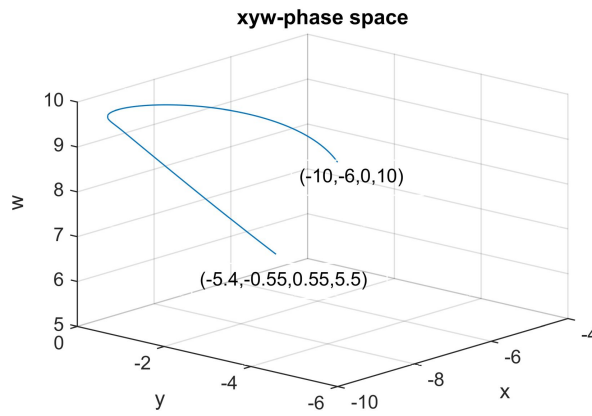


Fig. 3.13. The xyw phase space after control at $eq2$.

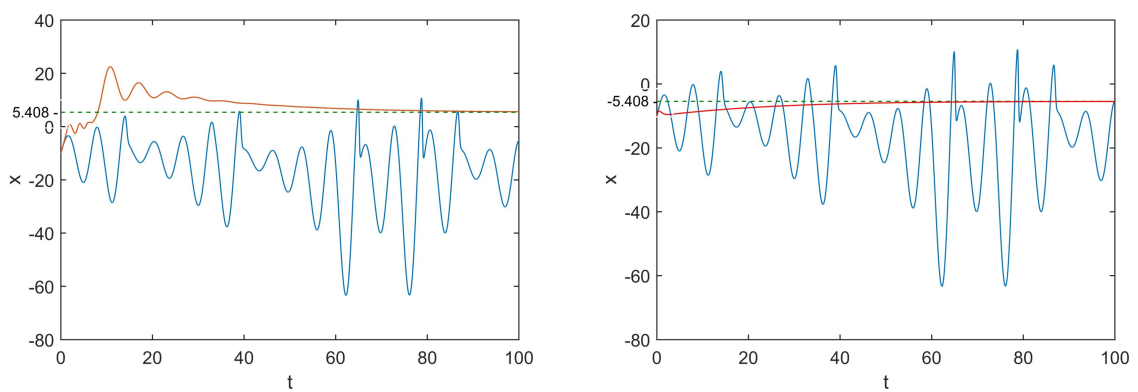


Fig. 3.14. The x trajectory behavior before control blue colored trajectory and after control red colored trajectory compared to $eq1$ and $eq2$ in green respectively.

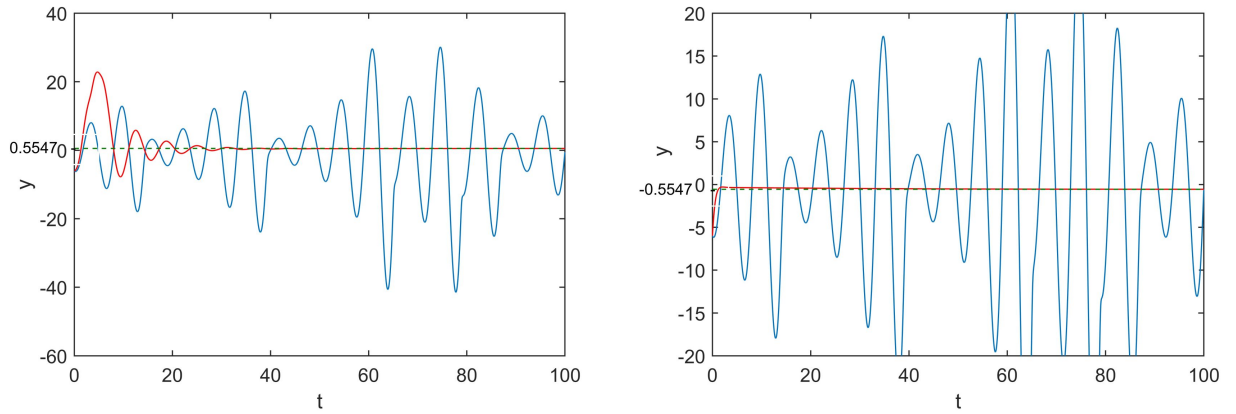


Fig. 3.15. The y trajectory behavior before control blue colored trajectory and after control red colored trajectory compared to $eq1$ and $eq2$ in green respectively.

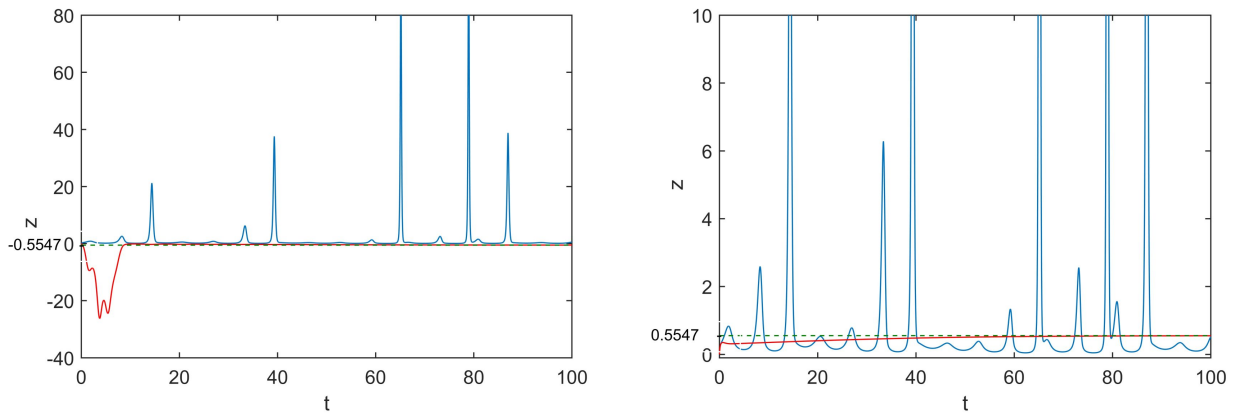


Fig. 3.16. The z trajectory behavior before control blue colored trajectory and after control red colored trajectory compared to $eq1$ and $eq2$ in green respectively.

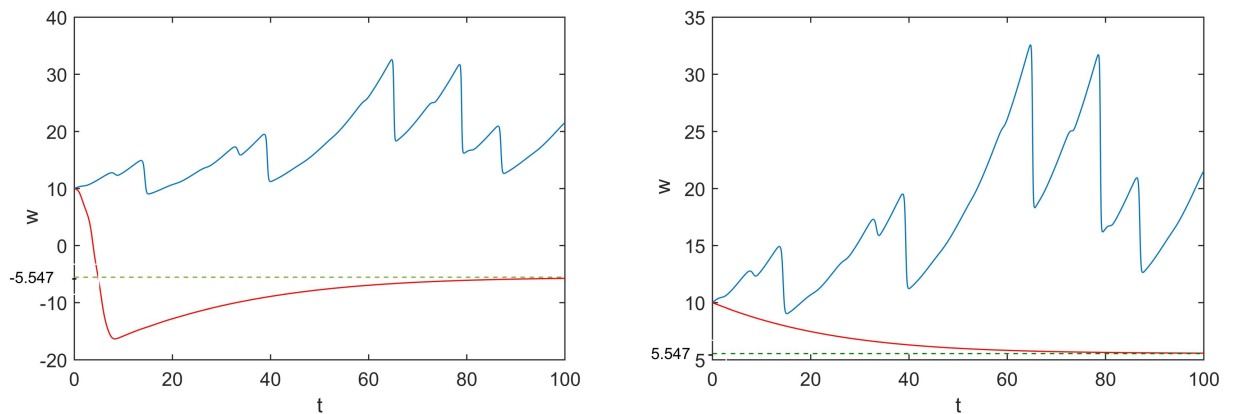


Fig. 3.17. The w trajectory behavior before control blue colored trajectory and after control red colored trajectory compared to $eq1$ and $eq2$ in green respectively.

4. CONCLUSION

In this paper, we have extended PFC method to stabilize chaotic continuous time systems by discretizing the system numerically using Euler method, and then applying the PFC method. The PFC method is used by adding small control term to the iterative solution of the system, this term is the multiplication of a controlling matrix by the difference between two consecutive predicted iterates. We have also discussed the stability analysis of the continuous system compared to its numerical discrete form, and the choice of the control matrix due to the eigenvalues of the discretized system type either real or complex, and we have proved that the method is stable. The method has been applied to the most popular systems, Lorenz 3D system and Rössler hyperchaos 4D system. Their trajectories have been controlled to each equilibrium point after a few iterations. The extended PFC method is easy implemented and highly efficient method for all chaotic systems to be stabilized, as we have generalized PFC method for all chaotic systems either discrete or continuous time system.

ACKNOWLEDGEMENTS

It is my pleasure to have the supervision of Prof. B. T. Polyak. And I would like to express my gratitude to him, for the patient guidance, support and advice he has provided me in this work. Also we would like to express our thankful to the editor and anonymous reviewers of the journal, for their great efforts and valuable revision.

REFERENCES

1. Andrievskii, B. R. & Fradkov, A. L. (2003) Control of Chaos: Methods and Applications. I. Methods. *Automation and remote control*, **64** (5), 673–713.
2. Boukabou, A. & Mansouri, N. (2008) Predictive Control of Continuous Chaotic Systems. *Int. J. Bifurcation Chaos*, **18** (2), 587–592.
3. Celka, P. (1994) Experimental verification of Pyragas Chaos Control method applied to Chua circuit. *Int. J. Bifurcation Chaos Appl. Sci. Eng.*, **4** (6), 29–36.
4. De Sousa Vieira, M. & Lichtenberg, A.J. (1996) Controlling chaos using nonlinear feedback with delay. *Phys. Rev. E*, **54** (2), 1200–1207.
5. Khalil, H. K. (2002) Nonlinear systems. Upper Saddle River, NJ: Prentice Hall.
6. Kostelich, E. J., Grebogi, C., Ott, E. & Yorke J. A. (1993) Higher-dimensional targeting. *Phys. Rev. E*, **47** (1), 305–310.
7. Lai, Y.-C., Ding, M. & Grebogi, C. (1993) Controlling hamiltonian chaos. *Phys. Rev. E*, **47** (1), 86–92.
8. Leonov, G. A., Zvyagintseva, K. A. & Kuznetsova, O. A. (2016) Pyragas stabilization of discrete systems via delayed feedback with periodic control gain. *IFAC-PapersOnLine*, **49** (14), 56–61.
9. Lorenz, E. (1963) Deterministic non-periodic flow. *Journal of the Atmospheric Sciences*, **20** (2), 130–141.
10. Mitsubori, K. & Aihara, K. (2002) Delayed–feedback control of chaotic roll motion of a flooded ship in waves. In *Proceedings of the Royal Society of London A: Mathematical, Physical and Engineering Sciences*, **458** (2027), 2801–2813.
11. Morgul, O. (2003) On the Stability of Delayed Feedback Controllers. *Phys. Lett. A*, **341**(4), 278–285.
12. Ott, E., Grebogi, C. & Yorke, J. A. (1990) Controlling Chaos. *Phys. Rev. Lett.*, **64**(11), 1196–1199.
13. Polyak, B. T. (2005) Stabilizing Chaos with Predictive Control. *Automation and Remote Control*, **66**(11), 1791–1804.

14. Pyragas, K. (1992) Continuous Control of Chaos by Self-Controlling Feedback. *Phys. Lett. A*, **170** (6), 421-428.
15. Pyragas, K. (1995) Control of Chaos via Extended Delay Feedback. *Phys. Lett. A*, **206**(5-6), 323-330.
16. Pyragas, K. (2006) Delayed feedback control of chaos. *Philosophical Transactions of the Royal Society of London A: Mathematical, Physical and Engineering Sciences*, **364**(1846), 2309–2334.
17. Schöll, E. & Schuster, H. G.(2008) *Handbook of chaos control*, John Wiley & Sons.
18. Ushio, T. (1996) Limitation of Delayed Feedback Control in Nonlinear Discrete-Time Systems. *IEEE Trans. Circ. Syst.*, **43**(9), 815–816.
19. Ushio, T., and Yamamoto, S. (1999) Prediction-based Control of Chaos. *Phys. Lett. A*, **264**(1), 30–35.